Influence of the transient conditions on release of corrosion products and oxidation of alloy 690 tubes during pressurized water reactor restart after steam generators replacement

Julie Flambard[a], Florence Carrette[a], Carole Monchy-Leroy[a], Eric Andrieu[b], Lydia Laffont[b,*]

[a] EDF R&D, Lab Les Renardières, Avenue des Renardières, Ecuelles – 77818 Moret-Sur-Loing Cedex– France
[b] CIRIMAT, Université de Toulouse, ENSIACET, 4 allée Emile Monso, BP 44362, 31077 Toulouse Cedex 4 – France

Keywords:
Alloy 690
Steam generator tube
Primary circuit (PWR)
Release
Oxidation

A B S T R A C T

The radioactivity of the Reactor Coolant System (RCS) of Pressurized Water Reactors (PWRs) mainly comes from the release of corrosion products of Steam Generator (SG) tubes made of Ni-base alloys. In order to reduce this activity and thus the radiation exposure of PWR operators during maintenance operations, it is necessary to minimize the release. That requires prior understanding of the various mechanisms involved. EDF R&D constructed a loop, BOREAL, to specifically measure rates of release of SG tubes in various conditions of primary environment. Tubes were usually tested at high temperature, under constant conditions of primary chemistry. So, it is necessary to carefully investigate the impact of transient conditions during a PWR restart after SG replacement. Tests were performed on the industrial material with curvature, roughness, defects and heterogeneities, regularly observed on this type of component. Characterisations of the inner surface were done on as-received and corroded specimens of SG tubes and were correlated with the obtained release kinetics.

The native oxide layer is formed of a very thin layer (1-2 nm) of oxidised matrix, without specific enrichment. During the restart, the most critical step for the release phenomenon is revealed from 170°C to 297°C. The majority of the metal is indeed released into the fluid during this step. The characterisations after release tests have made it possible to propose oxidation and release mechanism during a PWR restart after SG replacement. Up to 170°C, a thin layer of amorphous chromium oxide is formed by selective dissolution of iron and nickel. When the temperature rises, this chromium oxide layer is not stable enough to be protective and the diffusion phenomena are activated. At 325°C, the oxide does not exhibit any particular enrichment and corresponds to an oxidised metal layer; an equilibrium is established and the rate of release reaches a pseudo-stationary regime.

1. Introduction

An important part of the activity and the contamination of the Reactor Coolant System (RCS) of Pressurized Water Reactors (PWRs) mainly originates from the activation of corrosion products released by the very large surface area of Steam Generator (SG) tubes made of nickel base alloys (alloy 600 ~ 75% Ni, 15% Cr, 10% Fe, alloy 690~ 60% Ni, 30% Cr, 10% Fe). The released isotope ^{58}Ni is activated into the isotope ^{58}Co that contaminates all the surfaces of the RCS. In order to reduce this radioactivity and hence the radiation exposure during the maintenance and associated operation costs, it is necessary to control and minimize the release. To achieve this goal, it takes in advance an adequate understanding of the various mechanisms involved. The oxide film formed on the nickel base alloys plays a key role in nickel release, as well as the PWR primary environment and the material characteristics that can also influence the oxide growth [1,2]. The oxide film formed under PWR conditions, at high temperature in nominal primary water (~ 1000 ppm Boron, ~ 2 ppm Lithium, ~ 20-30 cm^3/kg NTP Hydrogen), is usually described as a duplex oxide layer with a compact inner layer enriched in chromium and a discontinuous outer layer that contains mainly, according to the tests facility, nickel ferrite, nickel chromite and nickel hydroxide [3,4,5]. Therefore, the chromium rich layer is considered to be the main factor of corrosion resistance of these alloys. Some authors suggest that, at high temperature, nickel base alloy behaviour regarding the

* Corresponding author at: CIRIMAT, Université de Toulouse, CNRS, INPT, UPS, ENSIACET, 4 allée Emile Monso, BP 44362, 31030 Toulouse Cedex 4, France
E-mail address: lydia.laffont@ensiacet.fr (L. Laffont).

https://doi.org/10.1016/j.jnucmat.2020.152562

oxidation and the release depends on the first stage of oxidation [6].

Several models were proposed to explain the mechanisms of oxidation and/or release of corrosion products in the primary environment. These models assume the duplex microstructure of the growing corrosion scale and also a continuous, uniform and homogeneous layer of oxides over the entire surface of the material. Furthermore, they consider additional assumptions about transport phenomena within the scale [7-9], dissolution of the scale [9,10], pore blocking and precipitation [8,10]. For example, the model of proposed by Gardey [11], essentially from electropolished wafers, combines the previous models of Robertson [9], Evans [8] and Lister [10] and considers the growth of a corrosion scale consisting of three different layers, the compact innermost layer acting as a diffusion barrier while the external layer is porous. The presence of pores in the oxide, which does not seem to be yet experimentally validated, is also mentioned. The model of Carrette [5,12] is based on characterisations of oxide layers, and underlying material, essentially formed on polished, electropolished and cold-worked wafers and a few SG tubes in primary medium at 325°C, on corrosion/release tests carried out on the same previous samples in primary medium à 325°C and with the use of tracers (D_20 and Xe) [5]. It considers phenomena of diffusion, space charges and dissolution. The work of Machet [6] on the oxide layers formed during the first oxidation times on 600 and 690 mirror polished alloys (wafers and flattened SG tubes), excludes a growth of parabolic type, associated with a purely diffusional mechanism. Moreover, all these models are based on tests conducted at high temperature, around 300 - 325°C, they do not integrate what might happen at lower temperatures. Finally, the majority of these models were established on tests carried out on model samples (mirror polished or even electropolished wafers, mirror polished flattened SG tubes) and none of these models makes it possible to account for the influence of the parameters of materials or linked to the medium, on the kinetics of corrosion and release.

EDF R&D has designed and built a specific loop, named BOREAL, to continuously measure release rates of SG tubes in various primary water conditions of PWRs [13]. The BOREAL loop reproduces the chemical, thermal and hydraulic conditions of the PWR primary water. Two types of parameters have an impact on the release phenomenon: the thermochemical conditions of primary water [4,10,13,14] and the internal surface state of SG tubes [2,15,16]. Release tests were usually performed on alloy 690 tubes (that replace alloy 600 tubes) at high temperature (285 – 325°C), under constant conditions of primary chemistry. For a better understanding of the release phenomenon, it is necessary to carefully investigate the impact of transient phases like start-up conditions of a reactor. During a restart of reactor, physico-chemical conditions significantly vary: pressure and temperature rise, boron and lithium concentrations change, hydrogen content increases, the primary fluid switches from oxidizing to reducing conditions. So, release tests were carried out with a temperature and chemistry program close to an actual reactor start-up on an industrial surface of SG tubes with their curvature, roughness, defects, and heterogeneities, regularly observed on this type of component and not on model samples. Considering a reactor restart after SG replacement, release tests were made on new tubes that is to say on non-oxidised tubes.

The objective of this paper is to present the impacts of temperature and chemistry transients, close to an actual reactor restart, on the oxidation and release of SG tubes in alloy 690. The aim of the study is to understand what happens in terms of release and oxidation of SG tubes during a restart after SG replacement, with the constraints of restart imposed by operations of reactors and operators. As a first step, release tests were performed in the BOREAL loop in order to simulate the transient phases of a reactor restart after SG replacement and to study the influence of chemistry and temperature on the release kinetics. In a second step, emphasis was put on the characterisation of the oxides formed during the corrosion tests, compared to the as-received tube surface state. These studies were performed using Scanning Electron Microscopy (SEM), Time-of-Flight Secondary Ion Mass Spectrometry (ToF-SIMS) and Transmission Electron Microscopy (TEM) as well as Scanning Transmission Electron Microscopy (STEM) coupled with Energy Dispersive Spectroscopy (EDS). These observations are correlated with release kinetics and provide a better understanding of the various implied mechanisms in the oxidation and release of corrosion products of SG tubes in alloy 690.

2. Materials and experimental methods

2.1. Test specimens

All tests were run with tube sections from a single steam generator tube made of alloy 690. The length of these specimens is 250 mm. The SG tube is of recent manufacturing, its outer diameter is 19.05 mm and its thickness is 1.09 mm. It was provided by Valinox Nucléaire and its heat number is HR282703. The bulk composition of the SG tube is given in Table 1.

The raw material undergoes initial hot transformations to obtain tube blanks. These blanks pass by a first transformation by cold rolling, followed by an intermediate recrystallization heat treatment under hydrogen at very high temperature. Then a second cold rolling transformation is carried out to obtain the steam generator tubes with a diameter of 19.05 mm and a thickness of 1.09 mm. After a sequence of cleaning and rinsing, the tubes undergo a final annealing heat treatment under hydrogen at 1060 - 1100°C with a severe cooling between 900 – 500°C to avoid precipitation of intragranular carbides. After a straitghtening operation to obtain the linearity criteria necessary for the assembly of the tubes in the steam generators, an additional heat treatment under vacuum at 715°C is carried out.

After manufacturing, no additional surface treatment was performed on the SG tube and its inner surface; tube sections used for the tests have an industrial inner surface state. Only before the tests, tube sections are cleaned under ultrasound with acetone, ethanol then ultrapure water.

2.2. Corrosion tests

The corrosion tests were carried out in the BOREAL loop [13] simulating primary water conditions. This equipment is a recirculating loop that reproduces chemical and thermo-hydraulical conditions of the primary fluid circulating inside SG tubing of PWRs. This facility is composed of plastics in the cold section and of zirconium or titanium alloys in the hot section, to avoid interference with the release of corrosion products of the SG tube tested. The use of Ultra Thin Layer Activation (UTLA) coupled with a gammametric detection allows to obtain, by continuous measurement, the kinetic of the release [17]. The release kinetic is expressed as the thickness of released metal as a function of the corrosion time and the sensitivity of detection is less than two nanometers in terms of thickness loss.

The tests reproduce as accurately as possible the temperature and chemistry (B, Li, pH, O_2, H_2) transients during a reactor restart. At the beginning, the aerated fluid is at room temperature (~ 25°C) without lithium and hydrogen but with boron (2500 ppm), the pH is of 4.6. The fluid is then deaerated from 60°C to decrease the content of oxygen until 5 ppb at 170°C. The oxygen content is in fact less than 10 ppb from 80°C. As part of the release tests in the BOREAL loop, this done by nitrogen injection. At 297°C, the boron

Table 1
Bulk composition of steam generator tubes made of alloy 690 in wt. %

Element	Ni	Cr	Fe	Al	Si	Ti	Mn	C	N	Co		
Wt. %	59.23	29.63	10.08	0.17	0.29	0.20	0.30	0.02	0.03	< 0.008	0.006	0,0002

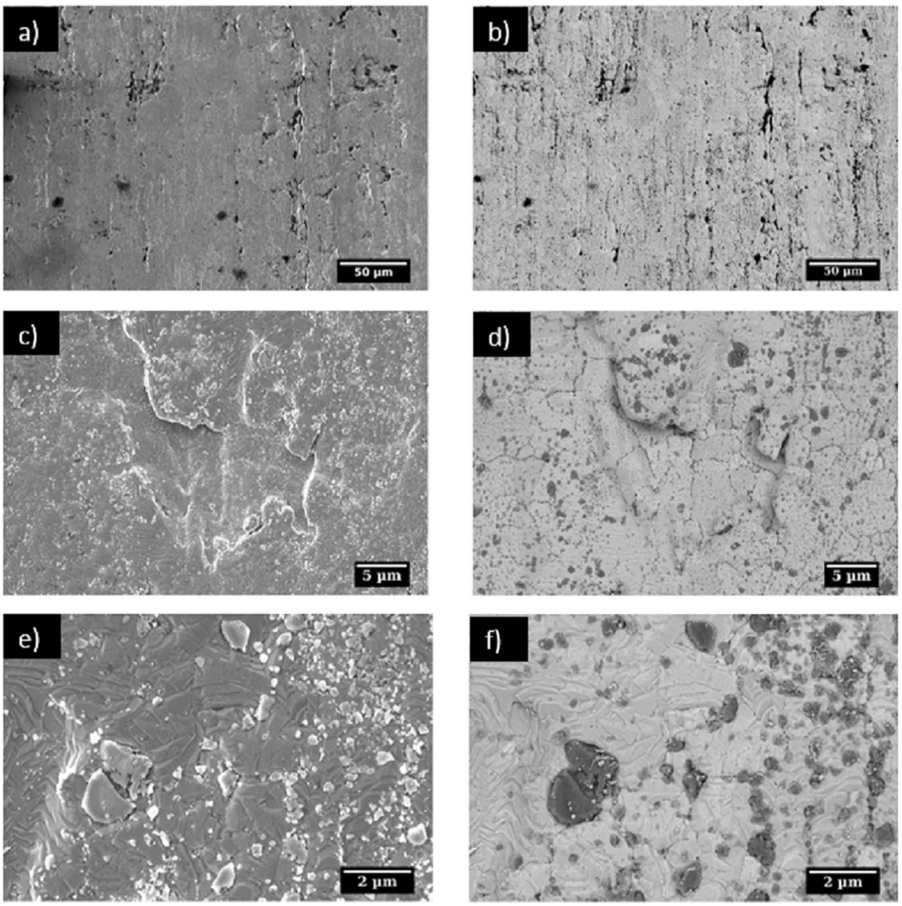

Figure 1. SEM images of 690 alloy steam generator tubes (inner surface) in as-received conditions in the secondary electrons mode (a, c, e) and in the backscattered electrons mode (b, d, f) respectively

concentration is reduced (2100 ppm), lithium (2.2 ppm) and hydrogen (5 - 20 cm^3/kg (NTP)) are injected. The calculated pH of the fluid at this temperature is of 6.6. At 306°C, the boron concentration is reduced (1600 ppm), lithium and hydrogen staying at the same concentrations (2.2 ppm, 5 – 20 cm^3/kg (NTP)), the calculated pH of the fluid at this temperature is of 6.9. The last section of the test is performed in nominal operating primary water at 325°C with a calculated pH of 7.3 (B = 1200 ppm, Li = 2.2 ppm, H_2 = 25 – 35 cm^3/kg (NTP)). From 25°C to 325°C, there are several transients that vary from a few hours to a few days.

2.3. Characterisations

The internal surface state of the tube and the oxides formed after the corrosion tests were observed by SEM. The SEM observations were carried out on a ZEISS Sigma microscope, at 5 kV using various magnifications and modes. The difficulty of the study is the preparation and the observation of an industrial surface, with defects, roughness, angle of curvature. Due to these difficulties, the cross-sections were prepared using ion polishing system (Ilion 2 GATAN). To protect the oxide, the sample was coated with gold before the cross-section.

Samples for TEM observations were prepared using a FEI Dual Beam HELIOS nanolab 600. TEM foils were further thinned and cleaned in a Precision Ion Polishing System (PIPS II) until the desired thickness was reached. Doing so, the artefacts induced during the lamellae extraction and thinning in the FIB were erased [18]. TEM analyses were made to investigate the oxide scale formed (thickness, morphological and chemical composition). TEM characterisations of the internal surface tube and the oxides were re-

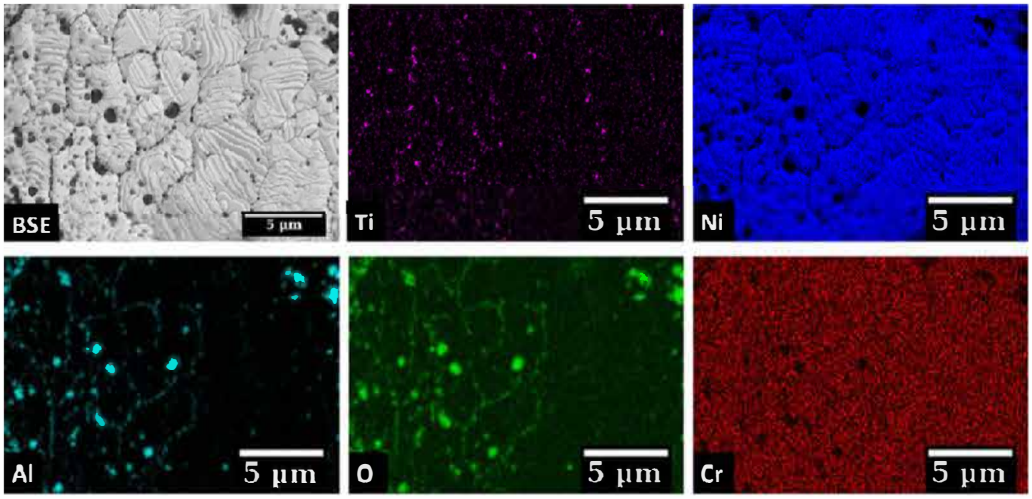

Figure 2. Backscattered SEM image and SEM EDX mapping (8kV) of alloy 690 steam generator tubes (inner surface) in as-received conditions

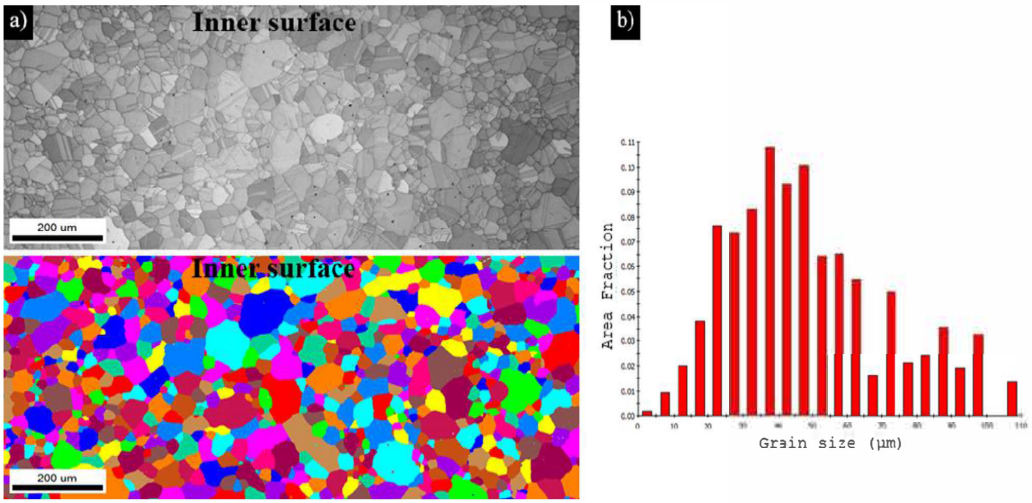

Figure 3. a) EBSD data treatment of 690 alloy steam generator tubes and b) histogram of grain size on EBSD data

alised using a FEI Tecnai Osiris 200 kV Scanning TEM (STEM) coupled with a Charge-Coupled Device (CCD) camera. This TEM was equipped with a Super-X SDD Energy Dispersive X-ray spectroscopy (EDXS) detector. A JEOL JEM 2100F with EDX detector (Bruker SDD Xflash 5030) and a JEOL ARM 200F with Cs corrector and EDX detector (JEOL CENTURIO SDD) were also used for STEM studies at UMS Castaing.

The oxide composition and the underlying material were also determined by using ToF-SIMS. ToF-SIMS data were acquired using a ToF-SIMS V spectrometer (Ion TOF). The sputtering was performed using a 2 keV (80 nA) Cs+ ion beam, rastered over an area of 300 × 300 μm^2. A 25 keV Bi^+ analysis beam was used to scan an area of 30 × 30 μm^2. The oxide sputtering rate was established assuming a constant rate, whatever the oxide composition (as the oxide density is always very similar), the resulting value is 0.321 ± 0.037 nm/s.

Following the intensity profile versus sputter time of specific oxide anions enable to evaluate the composition of the oxide layer whereas the intensity profile of Ni_2^- allows to determine the thickness of the layer [19]. Ni_2^- is representative of the metallic matrix and as soon as the profile of this ion reaches a constant value, one can assume that the base metal is reached. Table 2 summarizes the link between the representative oxide anions analysed by ToF-SIMS and the corresponding oxides.

3. Resultses

3.1. Initial characterizations of the as-received SG tube

In order to characterize the topography, different segments of the SG tube were tested with the as-received surface condition. The observations by SEM and EDS analyses of the internal surface

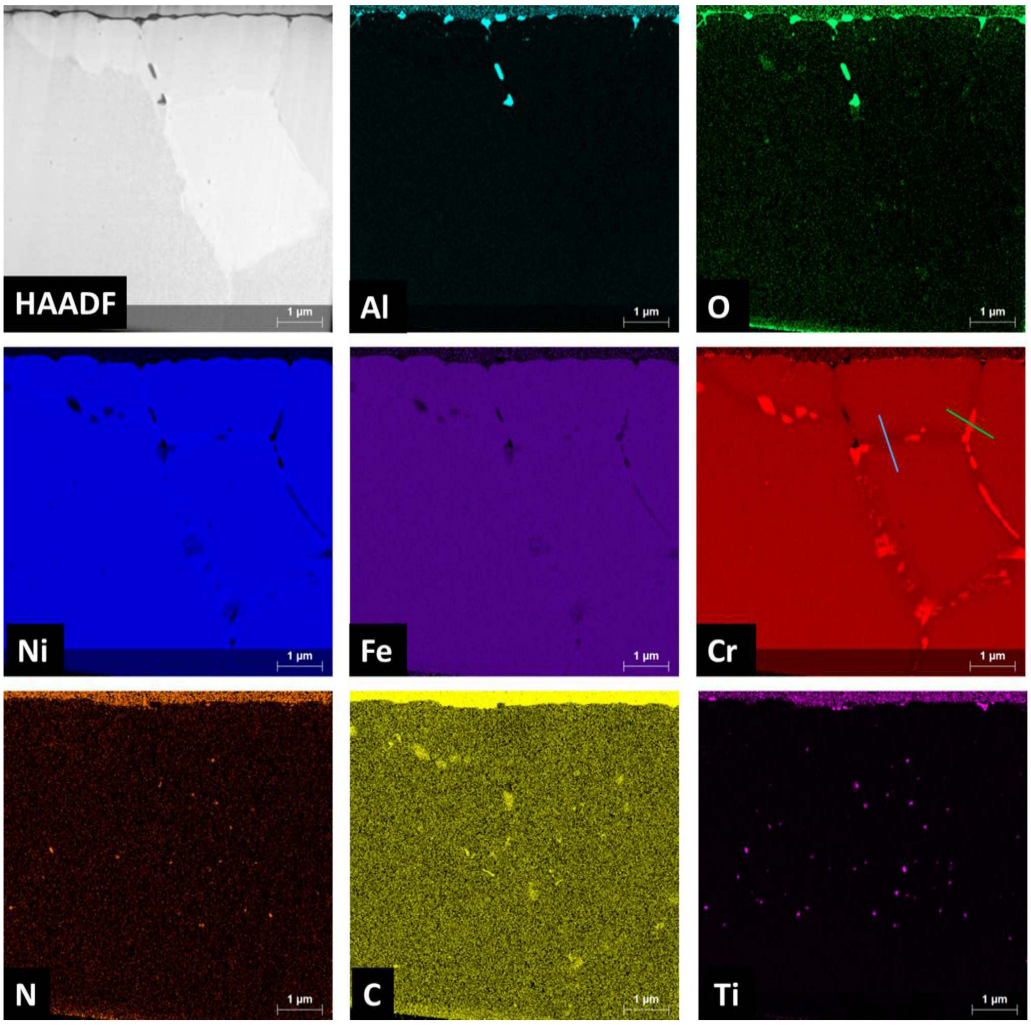

Figure 4. HAADF STEM image associated with STEM EDX mapping of 690 alloy steam generator tube (inner surface) in as-received conditions

Table 2
Oxide anions analysed by ToF-SIMS and the chemical species associated

Specific oxide anions	Chemical species associated
O_2^- et $^{18}O^-$	Oxides
OH^-	Hydroxides
$NiOH^-$	Nickel hydroxide
FeO^-	Iron oxide
NiO^-	Nickel oxide (NiO / Ni hydroxides)
CrO^-	Cr oxide (like Cr_2O_3)
CrO^{2-}	Cr_2O_3 / chromite $Ni_{(1-x)}Fe_{(x)}Cr_2O_4$
Ni^{2-}, Cr^{2-}, Fe^{2-}	Matrix Ni, Cr, Fe
TiO^-, TiO_2^-	Titanium oxide
AlO_2^-	Aluminium oxide

of virgin SG tube sections used for tests are presented on Figure 1 and Figure 2. The Figure 1 represents SEM images in secondary (a, c, e) and backscattered (b, d, f) electrons of different areas representative of the internal surface of the SG tube at different magnifications respectively. At the scale of characterisations or compared to mirror polished / electropolished specimens, the inner surface is pretty rough and disturbed with striations and folds parallel to the longitudinal axis of the tube, due to the manufacturing process, as we can see in Figure 1c and d. At the industrial scale for this type of material, the inner surface is nevertheless considered not rough; the roughness (Ra value) is of 0.3 µm (French guidelines specifying a Ra value inferior to 0.8 µm for the inner surface of SG tubes). In addition, studies showed that the Ra value seems to have no influence on release of corrosion products of SG tubes [20-22]. Numerous inclusions are observed as we can see in backscattered images (Figure 1b, d, f), grain boundaries are well defined.

In order to identify the inclusions, SEM EDX mappings of major elements (Ni, Cr, O, Ti, Al), possibly containing in the tube, are displayed in Fig. 2. Aluminium associated with the oxygen signal

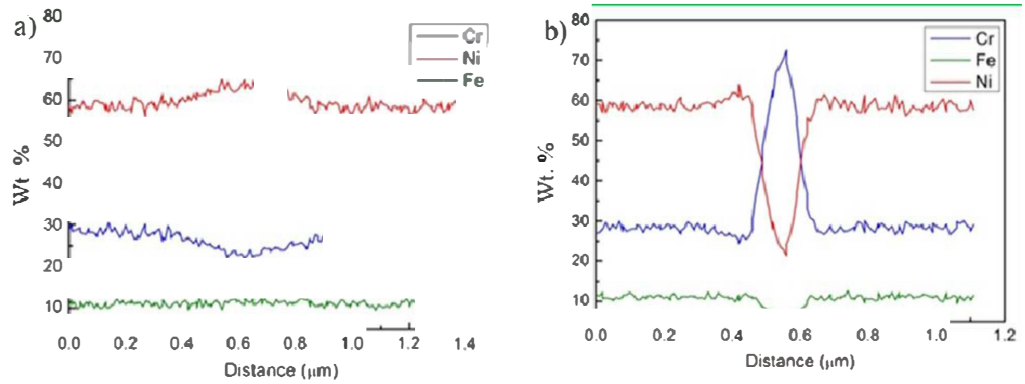

Figure 5. EDX linescan on a) chromium depletion and b) chromium carbide on 690 alloy steam generator tubes (inner surface) in as-received conditions

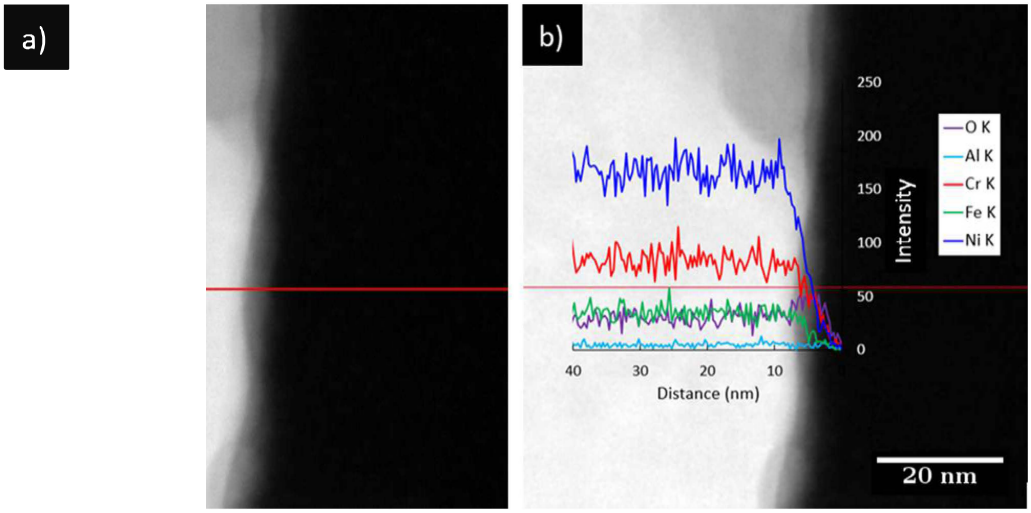

Figure 6. a) STEM HAADF image of the inner extreme surface of the steam generator tube on alloy 690 at the initial state and d) EDX compositional profiles of O, Al, Cr, Fe and Ni

shows the significant presence of inclusions of Alumina in the internal surface. Titanium traces, partially oxidised, are also detected, mainly at grain boundaries of the extreme surface.

Average grain size was obtained thanks to EBSD mapping and data treatments using the OIM analysis software (Fig. 3). The imposed misorientation for the grain calculation was of five degrees allowing to represent at best the grain population. The average grain size of the 690 alloy steam generator tubes is about 50 μm in the thickness of the tube. As previously observed on 690 alloy SG tubes [22], the structure is heterogeneous, there are small and large grain populations on all the tube thickness, it still respects French guidelines ($5 <$ conventional index of grain size $G < 9$). Data on 600 and 690 alloys demonstrated that, across the thickness of the material, a structure homogeneous with small grains or large grains or heterogeneous in terms of grain size has no influence on corrosion and release rates [11,15,21,22]. Nevertheless, these areas with very small grains but also with large grains at the extreme internal surface imply the opportunity of different behaviours concerning corrosion and release phenomena [22]. When very small grains of 1 – 2 µm diameter on a thickness of 2 µm maximum are present at the extreme surface, the release rate seems to be divided by a factor 2 [22]. The beneficial effect of this type of microstructure would come from increased diffusion of chromium to the surface via grain boundaries to form internal protective layer. This kind of microstructure at the extreme surface of SG tubes remains nevertheless very sporadic and it is preferable not recommended to avoid stress corrosion cracking.

To describe the inner surface state before oxidation, TEM characterisations were performed. The Fig. 4 shows HAADF STEM image of the internal surface of the tube where grain boundaries are present and STEM EDX mapping of the chemical elements of interest. The presence of aluminium oxide is visible up to 3 µm whereas titanium precipitates, in the form of TiN are also observed up to 6 µm. The presence of aluminium and titanium were already noted on the inner surface and in the bulk of SG tubes [22,23]. The Fig. 5 represents line profiles done in Fig. 4 along a grain boundary on a chromium carbide and between them. At grain boundaries, chromium carbides (Fig. 5b) and a slight depletion of chromium

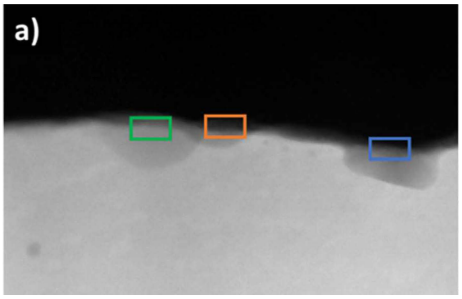

O	0	30,8	42,7
Cr	65,8	31,6	26,6
Ni	28,6	5,4	4,6
Fe	5,6	32,2	26,1

Figure 7. a) STEM HAADF image of the inner extreme surface of the steam generator tube on alloy 690 at the initial state and d) EDX analysis (at. %) of identified areas

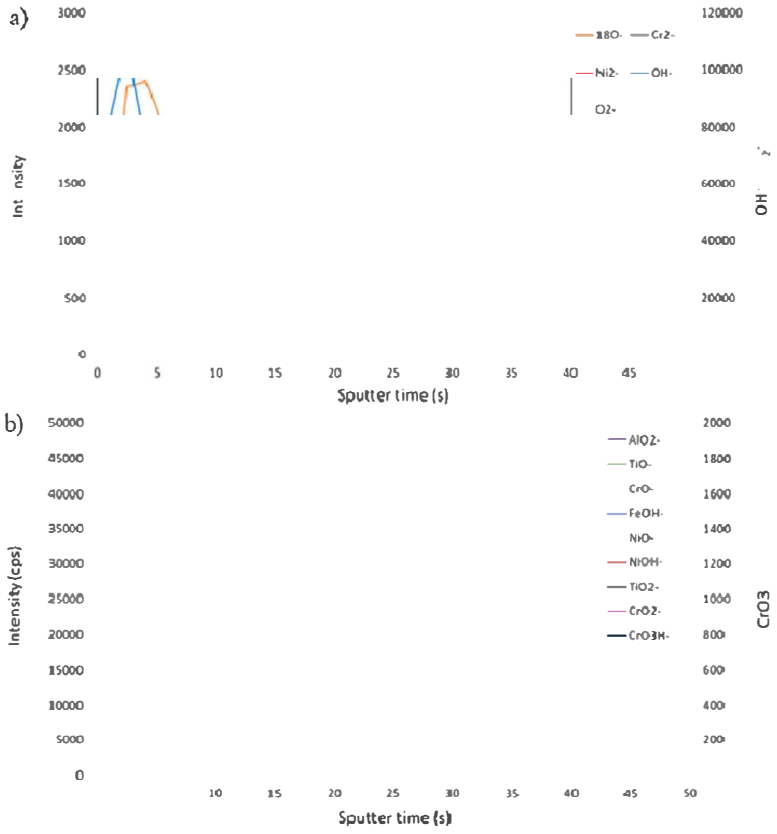

Figure 8. ToF-SIMS profiles of a) the specific oxide anions $^{18}O^-$, Cr_2^-, Ni_2^-, OH^- and O_2^- b) AlO_2^-, TiO^-, CrO^-, $FeOH^-$, NiO^-, $NiOH^-$, TiO_2^-, CrO_2^-, CrO_3H^- for the initial surface state of the steam generator tube on alloy 690

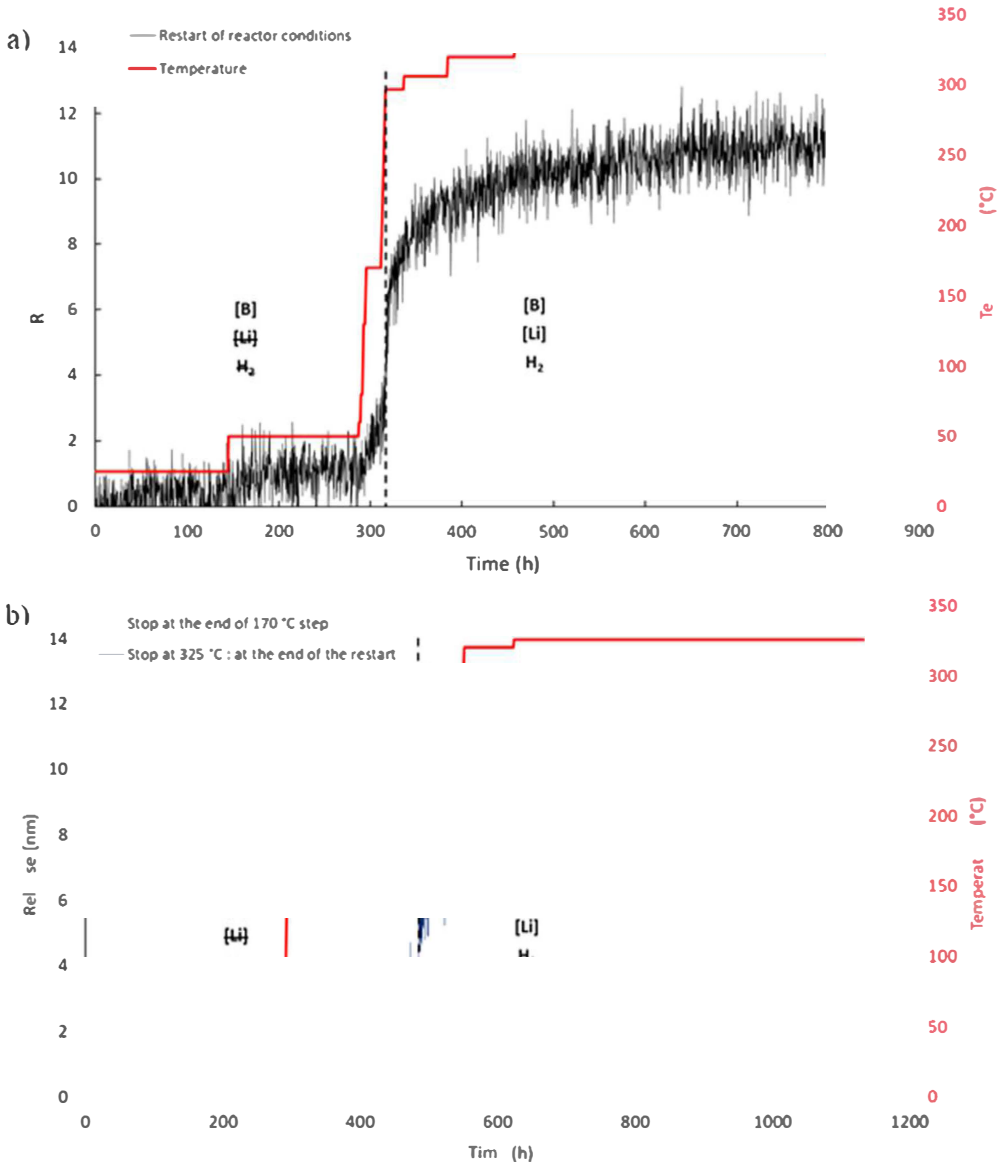

Figure 9. Release kinetics of the 690 alloy steam generator tube during transients tests simulating restart of reactor with change of chemistry and temperature a) until 325°C and b) step at 170°C during 200 hours until 170°C (for the orange) and until 325°C (for the blue)

between them along grain boundaries (Fig. 5a) are highlighted. The intergranular chromium carbides, formed during the manufacturing process, are significantly developed by thermal treatment. These chromium carbides, which protect Alloy 690 from stress corrosion cracking, are identified as $Cr_{23}C_6$ using selected area diffraction pattern (SAED) [24] and have a cube-cube relationship with the matrix [25].

The Fig. 6 presents a STEM HAADF image combined with an EDX profile from the surface of the oxide to the matrix. The native oxide layer does not seem to present a particular enrichment except for oxygen. It would correspond to a thin layer of oxidised matrix. The thickness of this native oxide layer is around 2 nm. In addition to this very thin oxide layer, small nodules are regularly observed along the surface. The Fig. 7 presents STEM HAADF image of the extreme surface of the tube combined with EDX analysis done on these small nodules (EDX boxes having the same size). EDX quantification (Fig. 7) reveals an area with an enrichment in chromium or just the oxidised matrix.

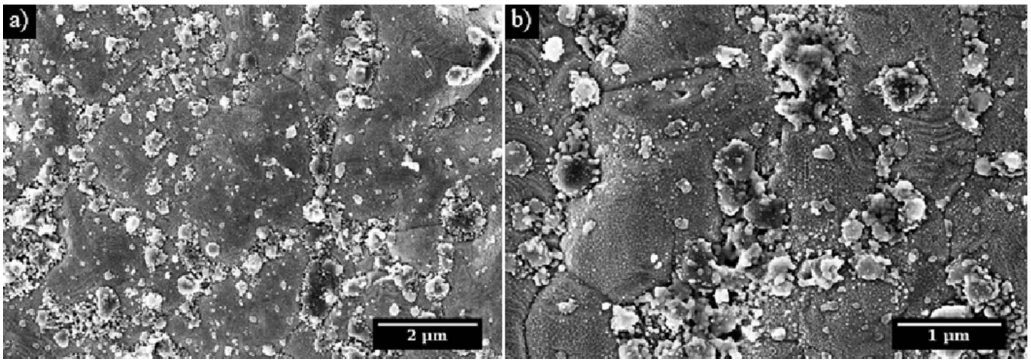

Figure 10. SEM images of oxides formed on the inner surface of steam generator tube made of alloy 690 corroded during transients test simulating restart of reactor until 170°C (image b obtained at higher magnification than image a)

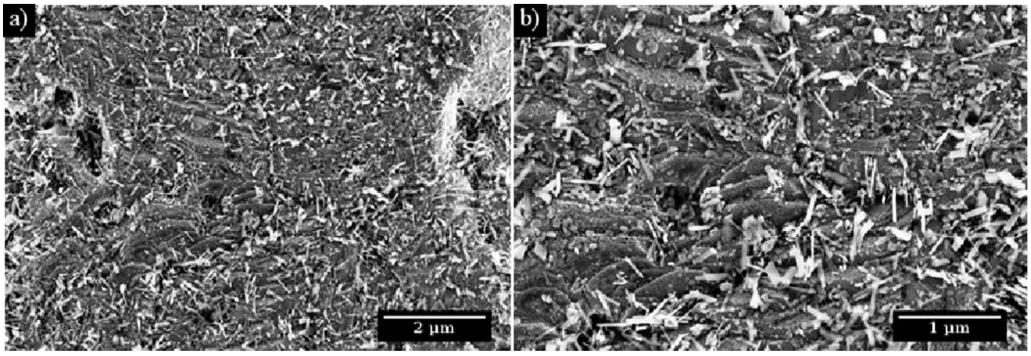

Figure 11. SEM images of oxides formed on the inner surface of steam generator tube made of alloy 690 corroded during transients test simulating restart of reactor until 325°C (image b obtained at higher magnification than image a)

ToF-SIMS analyses were performed to estimate the thickness and the chemical composition of the native oxide. Fig. 8 shows the ToF-SIMS profiles obtained on the initial surface state of the tube. The Ni_2^- signal reaches its maximum intensity after ≈ 8 s of sputtering corresponding to a native oxide layer thickness of ≈ 2-3 nm. A detailed examination of the different signals in the profiles provides more information. The inner extreme surface is characterised by intense hydroxides signals. Then the oxide signals, that reach their maximum intensity around 4 - 5 seconds of sputtering, demonstrate that the native oxide corresponds to oxidised matrix, without any enrichment of chemical element. The presence of Alumina and titanium oxide at the surface is confirmed. Beyond the oxide/metal interface, we can notice the slow decrease of MO_2^- and MO^- signals (M being a metallic cation) and the slow increase of the Ni_2^- signals. This effect may result from the very low roughness of the inner surface, due to the manufacturing of the SG tube.

The tube studied does not seem to have a gradient in chemical composition. However, a microstructure gradient is demonstrated with a heterogeneous grain size in the thickness of the tube and the presence of numerous inclusions and precipitates. The surface appears to be very disturbed, the grain boundaries are very well defined and steps, revealing the dense planes are visible at high magnifications. The oxygen-rich layer present in the initial state is very thin, 1 to 2 nm and no enrichment in a particular chemical element is highlighted.

One of the objectives of this study was to simulate as closely as possible the stages of a PWR restart on a new SG tube using the BOREAL loop and thus, to obtain the kinetics of release associated.

3.2. Release kinetics

The release kinetic of the 690 alloy SG tube during transient phases is presented in Fig. 9a. For remember, at the beginning, the aerated fluid is at room temperature without lithium and hydrogen but with boron (2500 ppm). Nitrogen is injected from 60°C to decrease the content of oxygen until 5 ppb at 170°C. At 297°C, the boron concentration is reduced (2100 ppm), lithium (2.2 ppm) and hydrogen (5 - 20 cm^3/kg (NTP)) are injected. During the first sections of the restart, about 300 hours at low temperature (25°C to 130°C), the release is very low. From 50°C, a slight release around 1 nm is noticeable on the kinetics. This is no very significant, however, this release indicates that the phenomenon begins to activate with this increase of temperature. Between 170°C and 297°C, a significant climb of the release is observed. The last section of the test, performed in nominal operating primary water (325°C, B = 1200 ppm, Li = 2.2 ppm, H_2 = 25 - 35 cm^3/kg (NTP)), shows a low release rate that decreases over time, reflecting the formation of the protective oxide layer. The oxide layer seems to be protective and stable. 11 nm of metal are released at the end of the test and a pseudo-stationary regime is established with a constant and low release rate of $2.4.10^{-3}$ nm/h (calculated between 600 and 800 hours of testing).

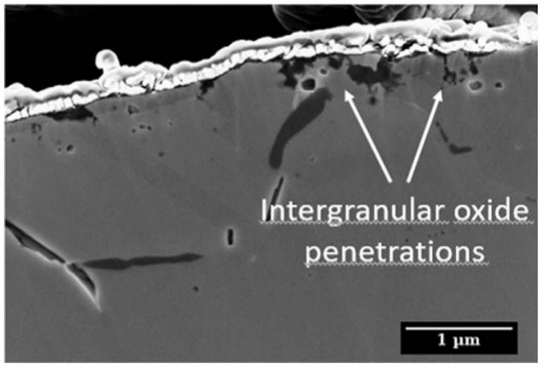

Figure 12. SEM images (cross-section) of intergranular oxide penetrations in the material on the inner surface of steam generator tube made of alloy 690 corroded during transients test simulating restart of reactor until 325°C

To improve the understanding of the release and oxidation phenomena around the critical temperature, a test was achieved until the step at 170°C (during 200 hours). Fig. 9b (orange curve) indicates that at this step, the released quantity is lower than the released quantity when the temperature rises 297°C. The final release is around 2 - 3 nm and the release rate calculated over the last 150 hours is $7.3.10^{-3}$ nm/h. When the test is continued until 325°C (blue curve), the kinetic is similar at the previous test, a significant climb of the release is observed between 170°C and 297°C. Then, in nominal operating primary water, the release rate is low and decreases over time. 10 nm of metal are released at the end of the test and a pseudo-stationary regime is established with a constant and low release rate of $2.4.10^{-3}$ nm/h. The duration of the step at 170°C does not have an impact on the final release.

To better understand the mechanisms implied in the release phenomenon, the inner surface of the SG tube sections have to be characterised after these transients tests.

3.3. Characterisation of the internal surface of the tubes after transients tests

The Figure 10 presents SEM images of the oxide on the inner surface of the SG tube corroded during transients tests until 170°C. This test was stopped just before the temperature rise 297°C, which means just before the significant climb of the release. The objective of these observations of oxides formed before the critical step, in term of release, is to better understand the evolution of the oxide formed during various stages of the reactor restart. The oxide appears to be relatively fine, the grain boundaries are always well defined, as observed on the as-received surface state. The steps revealing the dense planes seem to be erased, less visible than on the as-received state. Very small crystallites are appeared, they are quite homogeneously distributed on the surface.

The Fig. 11 presents SEM images of the inner surface of the SG tube corroded in conditions of restart of reactor until 325°C. The grain boundaries are well defined and seem to be more pronounced and steps are again well defined. The oxide layer is composed of sticks and needles shaped elements mainly observed at grain boundaries and on disturbed areas. At high magnification, the surface appears covered by very small nanometer sized crystallites. The small thickness of oxides and their heterogeneous aspect do not allow some analyses by EDX. In cross-section, limited intergranular oxide penetrations and small oxidised zones are also observed in Fig. 12, as already seen in the work of F. Carrette [21].

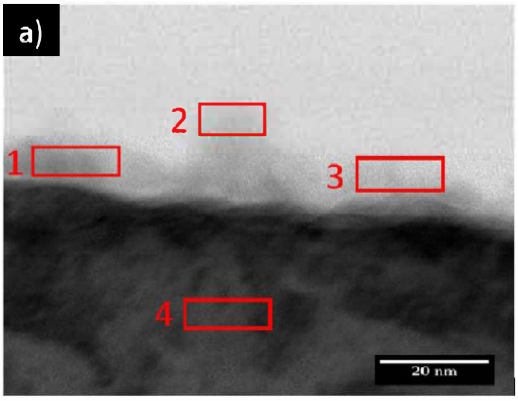

b)

	O	Cr	Ni	Fe
1	37	59	2	2
2	58	36	4	2
3	68	26	2	4
4	0	29	61	10

Figure 13. a) STEM image of the inner extreme surface of the steam generator tube on alloy 690 after transients test until 170°C and b) EDX analysis (at. %) of identified areas (red rectangles from 1 to 4)

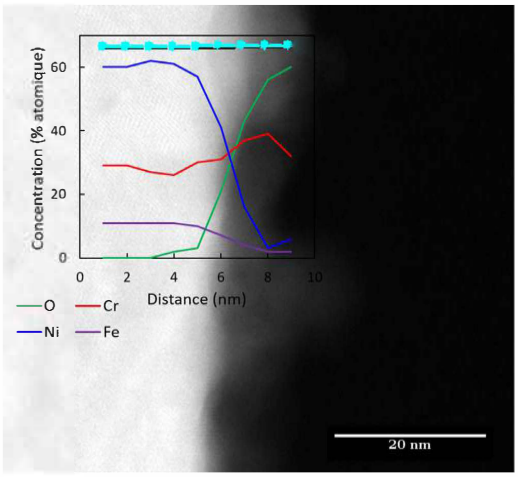

Figure 14. STEM HAADF image of the inner extreme surface of the steam generator tube on alloy 690 after transients test until 170°C and EDX compositional profiles along the matrix/oxide

After these SEM observations, the oxide layers are studied by STEM EDX after preparation of the samples by FIB in cross-section. This allows finer characterisations and chemical analysis of the oxide layer at the nano-scale. The average thicknesses of oxide layers are determined by several measurements carried out at different locations.

The Fig. 13 presents STEM bright field image of the extreme inner surface of the oxidised tube as well as chemical analyses carried out on the zones marked by rectangles, numbered from 1 to 4. The EDX analysis evidence that small crystallites (10 to 20 nm) observed on the surface appear to be highly enriched in chromium (rectangles 1, 2 and 3). The EDX linescan, presented in Fig. 14, con-

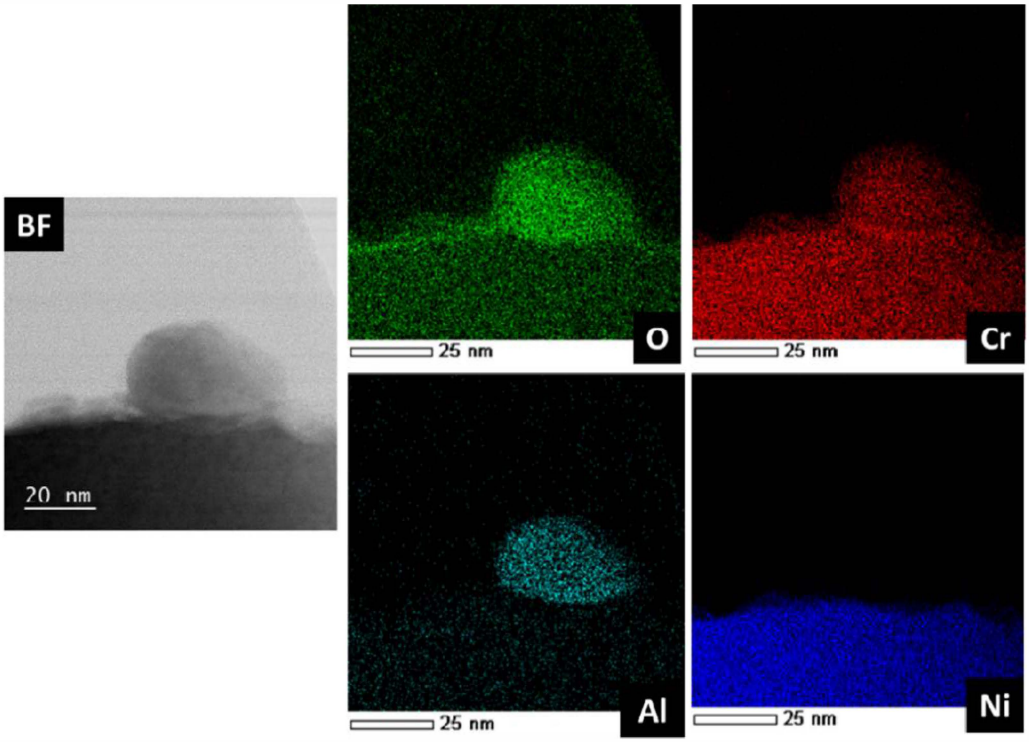

Figure 15. STEM bright field image and STEM EDX mappings of the oxide grown near an inclusion of Alumina on the inner extreme surface of steam generator tube on alloy 690 after transients test until 170°C

firm that the oxide is rich in chromium. The EDX profiles of iron and nickel fall sharply in the oxide while those of chromium and oxygen increase significantly.

So the oxide layer formed until the intermediate step at 170°C consists of a very thin layer of chromium oxide, with a thickness between 2 – 3 nm.

To better understand the formation of the oxide at the extreme surface on precipitates already present at initial state, chemical mapping was performed at the metal/oxide interface. The maps in Fig. 15 show the STEM EDX analysis around an Alumina inclusion initially present at the as-received state. Alumina inclusions are indeed always present at this temperature (170°C). STEM EDX maps of iron and chromium highlight the thin layer of chromium oxide on the surface of the sample as well as around the inclusion of Alumina. The inclusion of Alumina is covered and surrounded by a thin layer of chromium oxide.

The STEM bright field image combined with EDX maps of the essential chemical elements shown in Fig. 16 show a precipitate of titanium oxide, which was already present at initial state. This precipitate appears to be coated with chromium oxide and is topped by an aggregate of small nanometric crystallites of chromium oxide.

The Fig. 17 shows the montage of bright field TEM images of the internal surface of the steam generator tube corroded in conditions of reactor restart until 325°C. The surface is disturbed and it is not perfectly flat: annealing twins, formed during the heat treatment at the end of manufacturing, are observed. The oxides are slightly different from those formed until 170°C (described above) because of the presence of needles and sticks that are clearly visible as well as very small crystallites at the extreme surface.

Fig. 18 presents the STEM EDX maps on area with needles and sticks shape elements that can reach a size of 100 – 150 nm and appear to be chromium and nickel oxide and/or hydroxide. A continuous layer of oxide is visible and does not seem to present any particular enrichment. On the other hand, the small crystallites, which cover the surface, seem to be chromium rich. These oxide crystallites measure approximately between 5 – 20 nm. Alumina is not observed on the extreme surface on this sample, which indicates that it must be dissolved in the fluid at high temperature (between 170°C and 300°C). Fig. 19 shows STEM EDX maps focused on an intergranular oxide penetration, from a titanium oxide precipitate in the present case, as already observed by F. Meng et al. [23]. This titanium oxide is recovered by small crystallites of chromium oxides. In the intergranular penetration, the chromium oxides are present followed by metallic Ni.

Fig. 20 shows an EDX linescan superimposed to the STEM HAADF image of the inner extreme surface of the tube representing the chemical evolution of the oxide layer. This indicates an oxidised matrix layer, about 2 – 3 nm thick, and a chromium oxide crystallites at the extreme surface.

In addition, the extreme surface of the tube was also studied by STEM in bright field mode in Fig. 21. EDX chemical analysis were carried out on different areas of the oxide, which have the same dimension, numbered from 1 to 4. Nanometric crystallites are observed from 2 to 6 nm size and are composed of chromium oxide as shown in the analysis of area 1. A rather continuous layer of ox-

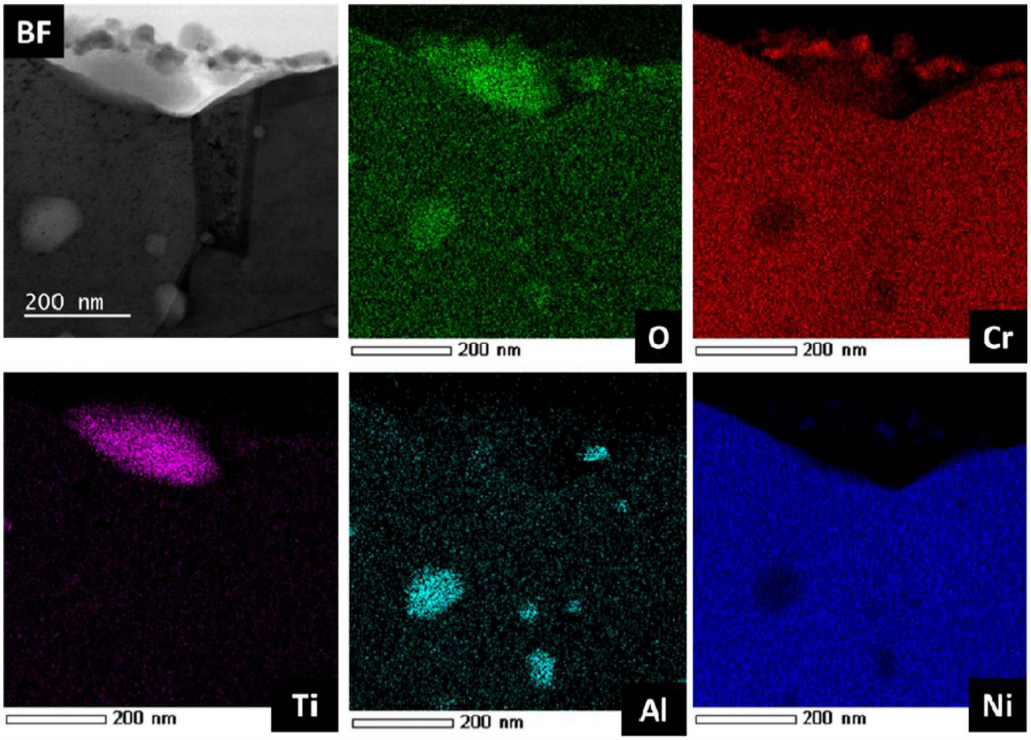

Figure 16. STEM bright field image and STEM EDX mappings of the oxide grown near a precipitate of titanium on the inner extreme surface of steam generator tube on alloy 690 after transients test until 170°C

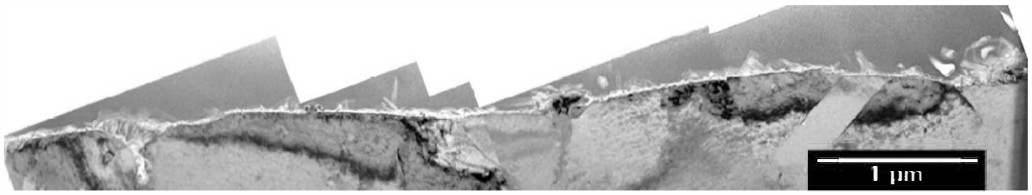

Figure 17. TEM bright field images of the oxide developed on the inner extreme surface of the steam generator tube in alloy 690 exposed in primary water during transients test until 325°C

ides is identified with a thickness between 2 and 5 nm. This layer corresponds to the oxidised matrix without any particular enrichment (EDX analyses of areas 2 and 3). The EDX analysis of area 4 corresponds to the chemical composition of the alloy 690.

The nature and chemical composition of the oxides were also studied by ToF-SIMS spectrometry. For both samples, ToF-SIMS profiles from the inner extreme surface to the material bulk were acquired.

Fig. 22 and Fig. 23 show the ToF-SIMS profiles obtained after transient's test in the BOREAL loop. For the test until 170°C (Fig. 22), the Ni_2^- signal reaches its maximum intensity after 23 seconds of sputtering corresponding to an oxide layer thickness of approximately 7 nm. A detailed examination of the different signals in the profiles provides more information. The extreme surface is characterised by intense hydroxides signals between 0 and 4 seconds of sputtering. Then the oxide signals, that reach their maximum intensity around 6 seconds of sputtering, demonstrate that the oxide is rich in chromium with characteristic ions of chromium oxide (CrO^-, CrO_2^-). The presence of Alumina and titanium oxide at the surface is always detected at this step of the transient.

For the test until 325°C (Fig. 23), the Ni_2^- signal reaches its maximum intensity after 150 seconds of sputtering corresponding to an oxide layer thickness of approximately 48 nm. The overestimate of the thickness is due to roughness induced by sticks and needles. The extreme surface is characterised by intense hydroxides signals between 0 and 20 seconds of sputtering, more precisely the chromium hydroxide thanks to CrO_3H^- signal. Therefore, this extreme surface area of the oxide layer is mainly composed of chromium hydroxide. In the internal part of this zone, the CrO_2^- signal increases strongly, corresponding to the chromium oxide present just below the hydroxide. The chromium oxide in contact with the fluid can be indeed in the form of hydroxide while the part which is not in direct contact is in the form of oxide.

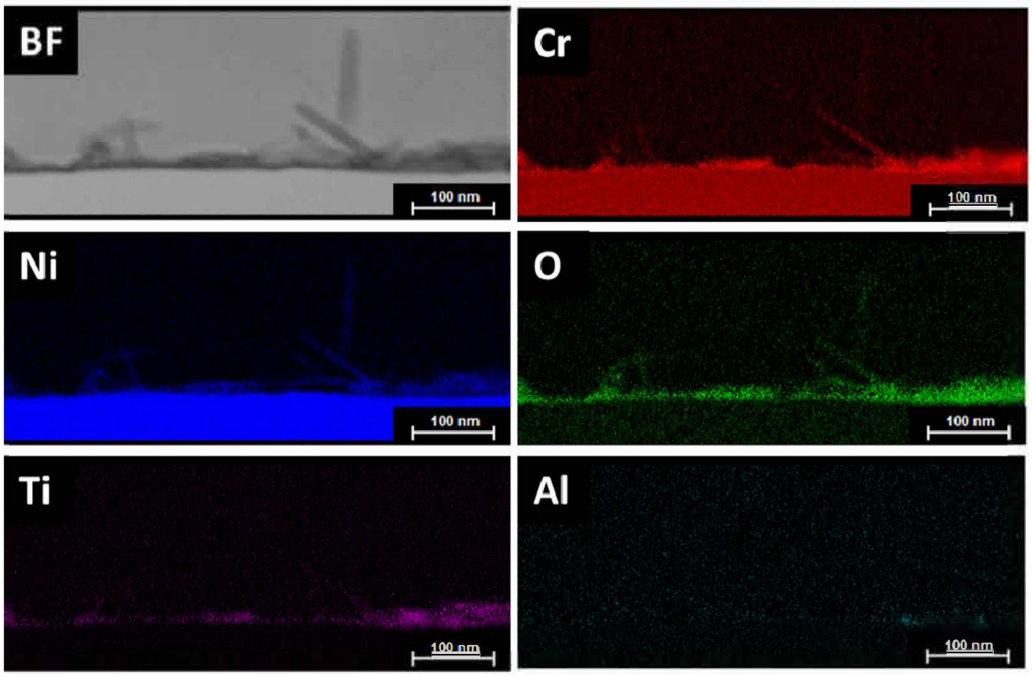

Figure 18. STEM bright field image and EDX mappings of the oxide grown on the inner extreme surface of steam generator tube on alloy 690 after transients test until 325°C

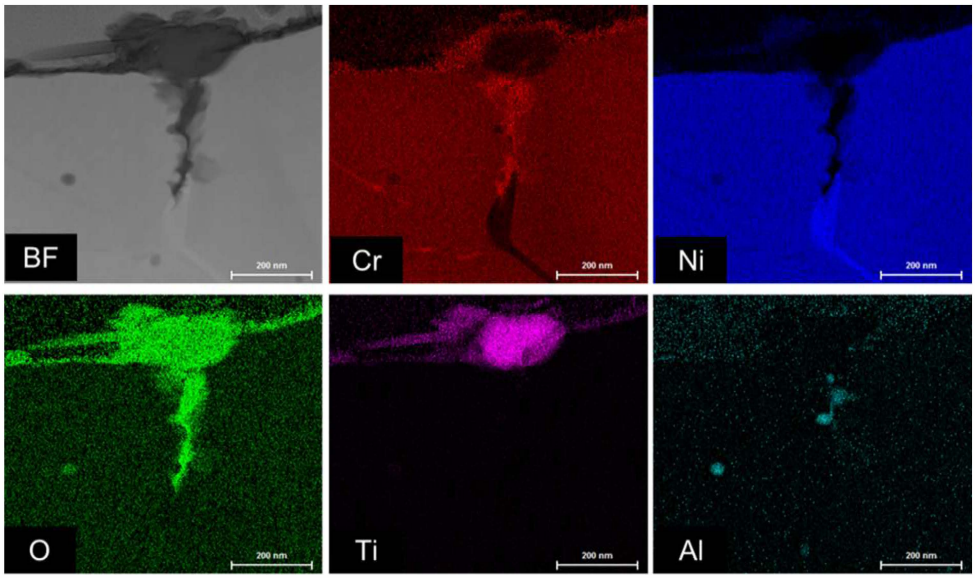

Figure 19. STEM bright field image and STEM EDX mappings of an intergranular oxide penetration at the level of a precipitate of titanium on the inner extreme surface of steam generator tube on alloy 690 after transients test until 325°C

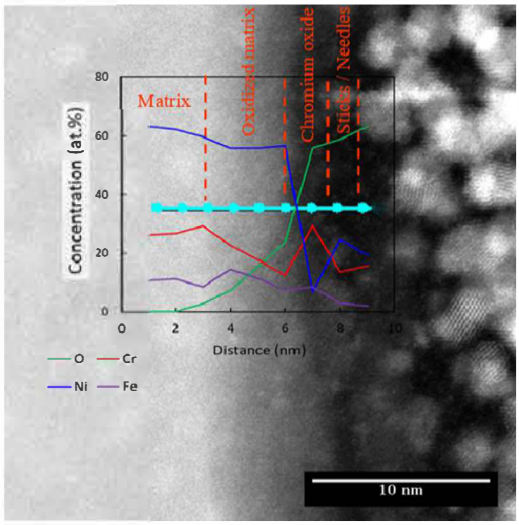

Figure 20. STEM HAADF image of the inner extreme surface of the steam generator tube on alloy 690 after transients test until 325°C superimposed to EDX compositional profiles

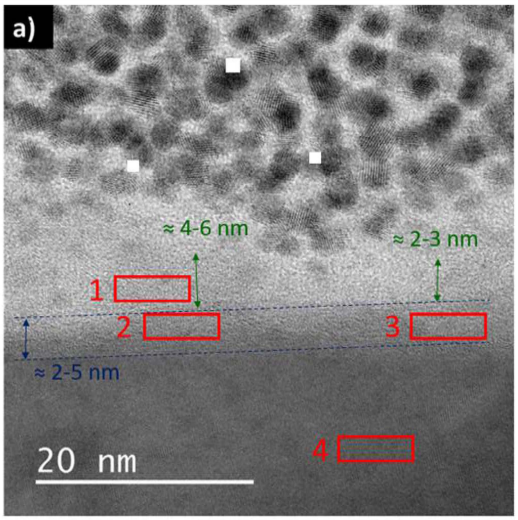

b)	O	Cr	Ni	Fe
1	62	29	7	2
2	20	19	54	7
3	21	21	51	7
4	1	28	61	10

Figure 21. a) STEM bright field image of the inner extreme surface of the steam generator tube on alloy 690 after transients test until 325°C and d) EDX analysis (at. %) of identified areas

More deeply, between 20 and 40 seconds of sputtering, the characteristic signals of the chromium, nickel and titanium oxides increase. The profiles have the same shape, which seems to indicate the presence of layer of oxidised matrix oxide, without particular enrichment. The presence of titanium oxide is always detected but not Alumina signal. The titanium signals can be explained by the significant presence of titanium at the extreme surface at the as-received state, which then can diffuse in the oxide layers during corrosion.

By looking in more detail at the metal/oxide interface, the interface is clearly characterised by a slow decrease of characteristic signals of the oxides and a slow increase of the Ni_2^- signal, characteristic of the metal. These are attributed to the formation of a rough interface resulting from the initial roughness of the surface of the sample and/or preferential oxidation with, for example, faster oxidation at the grain boundaries and disturbed areas. Therefore, these phenomena lead to the overestimation of the oxide thickness. However, the profiles are interesting and complementary to the observations made by microscopy. These analyses are rather coherent with previous observations.

4. Discussion

4.1. Evolution of the inner surface during the reactor restart after SGR

The experimental results presented above allow studying the effect of transient phases on the oxidation and the release of SG tubes. Fig. 24 shows the schematic drawings of the oxide on the nickel-based alloy after a restart of reactor (after steam generators replacement). For simplicity, the surface of the tube is shown plane, but it is important to remember that samples of tube are not planar. They are slightly rough with a heterogeneous structure (various inclusions, folds).

At the as-received state, an oxygen enriched layer with a thickness of 1 to 2 nm is highlighted. This oxide layer has no enrichment in a particular chemical element (Ni, Cr, Fe). The inner surface of the tube also has many inclusions of Alumina, which are exogenous particles coming from Corundum used during the manufacturing process. These inclusions, varying in size from 10 to 300 nm, are embedded on the surface of the tube and are observed up to 2 - 3 µm deep. Titanium precipitates, more specifically titanium nitrides, are also present up a depth of 5 - 6 µm, these precipitates are in the potential form of titanium oxides when they are close to the extreme surface.

At the end of the step at 170°C, so before the important rise of release during the BOREAL test, a thin layer of chromium oxide, with a thickness of 2 – 3 nm, is formed. The Alumina inclusions, present on the surface, are also covered with a thin layer of chromium oxide, this oxide surrounds the inclusion. The same phenomenon is observed around the titanium oxides at the extreme surface. Small crystallites (10 – 20 nm) of chromium oxide are observed on the extreme surface. The Alumina inclusions and the titanium oxide precipitates initially present are less embedded in the material. The precipitates located deeper in the material have not changed.

At the end of the test, once the full power conditions of reactor at 325°C are reached and maintained for 3 weeks, a layer of oxides of 2 – 5 nm is observed. This layer does not show any particular enrichment in a chemical element of the alloy. The nanometric chromium oxide crystallites are still observed, as at the end of the step at 170°C, it seems that their density is a little higher. Needles and sticks, with an average length of 100 – 150 nm and a thickness of a few nanometers, cover the surface with higher density at grain boundaries and disturbed areas. These specially shaped oxides appear to be composed of oxides and/or hydroxides of nickel and chromium. Alumina inclusions, which were in contact with primary water, are no longer observed. They are dissolved in the medium during the rise in temperature. Titanium oxide pre-

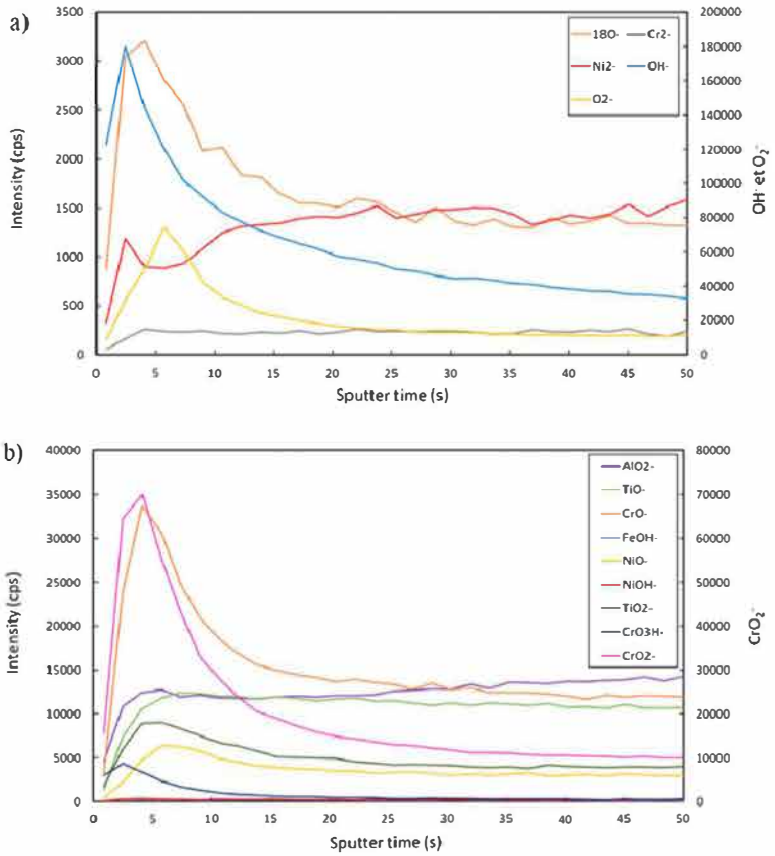

Figure 22. ToF-SIMS profiles of a) the specific oxide anions $^{18}O^-$, Cr_2^-, Ni_2^-, OH^- and O_2^- b) AlO_2^-, TiO^-, CrO^-, $FeOH^-$, NiO^-, $NiOH^-$, TiO_2^-, CrO_2^-, CrO_3H^- for the inner extreme surface of steam generator tubes made of alloy 690 corroded during transient's test until 170°C

cipitates are still present. The precipitates located deeper in the material have not changed.

4.2. Thermodynamic approach

Before the release tests and the characterisation of the internal surface of the tube sections after tests, oxides that can form thermodynamically during major transients from 25°C to 325°C were searched from literature data. Redox potential values and pH values (in temperature) were calculated by ChemworksTools (version 4.3.0) code with MULTEQ database (version 9) Data do not always exist for the different interesting transients of the present study that is to say at 25°C, 170°C, 297°C and 325°C. Calculations and stability diagrams of oxides which are likely to form during the exposition of Alloy 690 in nominal primary water at high temperature (conditions very closed to those of the present release tests: 1000 ppm boron, 2 ppm lithium, ~30 cm^3/kg (NTP) hydrogen) were established by Sennour *et al.* [3]. They reveal that, thermodynamically, formed oxides can be classified by stability rate in the following order: Cr2O3 > FeCr2O4 > NiCr2O4 > NiFe2O4 > NiO. Moreover, potential-pH diagrams of the Ni-Cr-Fe ternary system created for different temperatures (25°C, 100°C, 200°C and 300°C) by Beverskog *et al.* [26] give an indication of oxides likely to form during the different transients of temperature and chemistry though data are not fully representative of the real system, the hypothesis [Fe(aq)]=[Cr(aq)]=[Ni(aq)]=10^{-6} mol. being considered in calculations. Thus, thermodynamically stable species are summarised in Table 3.

The results of the different characterisations are not entirely in agreement with thermodynamic data. They mention the presence of iron as iron oxide whereas iron is not really detected in the analyses. Rather in ionic form, oxide layers are essentially composed of chromium oxide/hydroxide. Although in ionic form at low temperatures, nickel is rather oxidised as oxide/hydroxide than metallic at high temperature in the present reducing conditions. The differences observed between the results of the characterisations and thermodynamic data indicate that the material/fluid system is out of equilibrium. This is not surprising given the many temperature and chemistry changes from 25°C to 325°C with steps varying from a few hours, a few dozen hours to a few hundred hours for the last one à 325°C. Moreover, the predictions does not take into account in one hand the microstructural aspects of the inner surface state with the heterogeneities as Al and Ti detection, the role that they can play in the formation of the oxide scale (and in the release), the various interfaces that can be observed and in the other hand, the kinetic aspects of the different phenomena involved (dissolution, precipitation, release, diffusion ...).

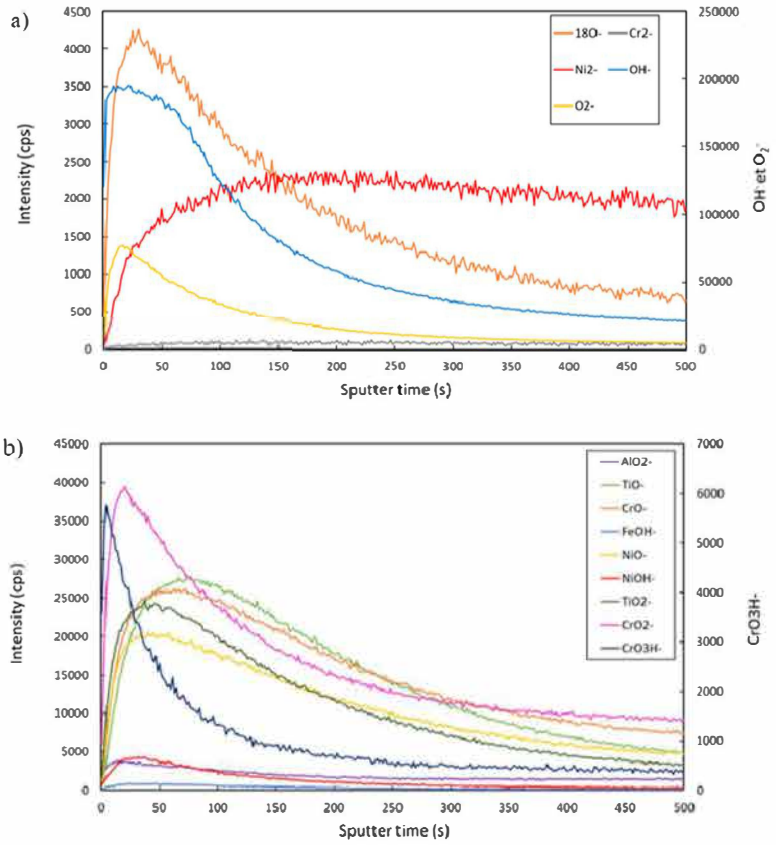

Figure 23. ToF-SIMS profiles of a) the specific oxide anions $^{18}O^-$, Cr_2^-, Ni_2^-, OH^- and O_2^- b) AlO_2^-, TiO^-, CrO^-, $FeOH^-$, NiO^-, $NiOH^-$, TiO_2^-, CrO_2^-, CrO_3H^- for the inner extreme surface of steam generator tubes made of alloy 690 corroded during transient's test until 325°C

Table 3
Synthesis of oxides/hydroxides thermodynamically stable during transients of a PWR restart for SG tubes in Ni-base alloys.

Thermochemical data of release tests													
Temperature (°C)	25		50	80		130		170	297		306		325
O_2/ H_2 presence	8 ppm	- -	O_2	10 ppb	O_2	-	→	5 ppb	5 cm^3/kg	-	H_2	→	35 cm^3/kg
Eh (V/ENH)	+ 0.942			→				+0.614	-0.685		→		-0.834
B/Li (ppm)	2500/0			-				2500/0	2100/2.2	→			1200/2.2
$pH_{(T°C)}$		4.6		→			4.7		6.6 – 6.7		→		~ 7.3

Thermodynamically stable oxides/hydroxides				
Temperature (°C)	25	100	200	300
Eh (V/ENH)	+0.942	+0.761	+0.551	-0.691→-0.726
$pH_{(T°C)}$	4.6	4.6	4.7	6.7
Oxides/Hydroxides	Fe_2O_3	Fe_2O_3	Fe_2O_3	$FeCr_2O_4$
	$HCrO_4^-$	$HCrO_4^-$	$HCrO_4^-$	$FeCr_2O_4$
	Ni^{2+}	Ni^{2+}	Ni^{2+}	Ni/NiO→Ni

4.3. Experimental approach

The description of oxides formed on the 690 alloy in primary water is quite far from the descriptions usually available in the literature for 600 (Mill Annealed and Thermal Treated) and 690 alloys. The internal chromium enriched oxide layer at 325°C is not observed. The origin of this observation is probably due to the test conditions. In particular, two major differences can be noted. The first concerns the material of the study. The tests of this study were carried out on the industrial component without modification of its geometry and especially of the internal surface state whereas almost all of the studies in the literature used model materials such as plates/wafers with surfaces most often flat and controlled (polished or even electropolished) which do not integrate or do not integrate anymore the effects of surface heterogeneities in terms of chemical composition and microstructure. The second concerns

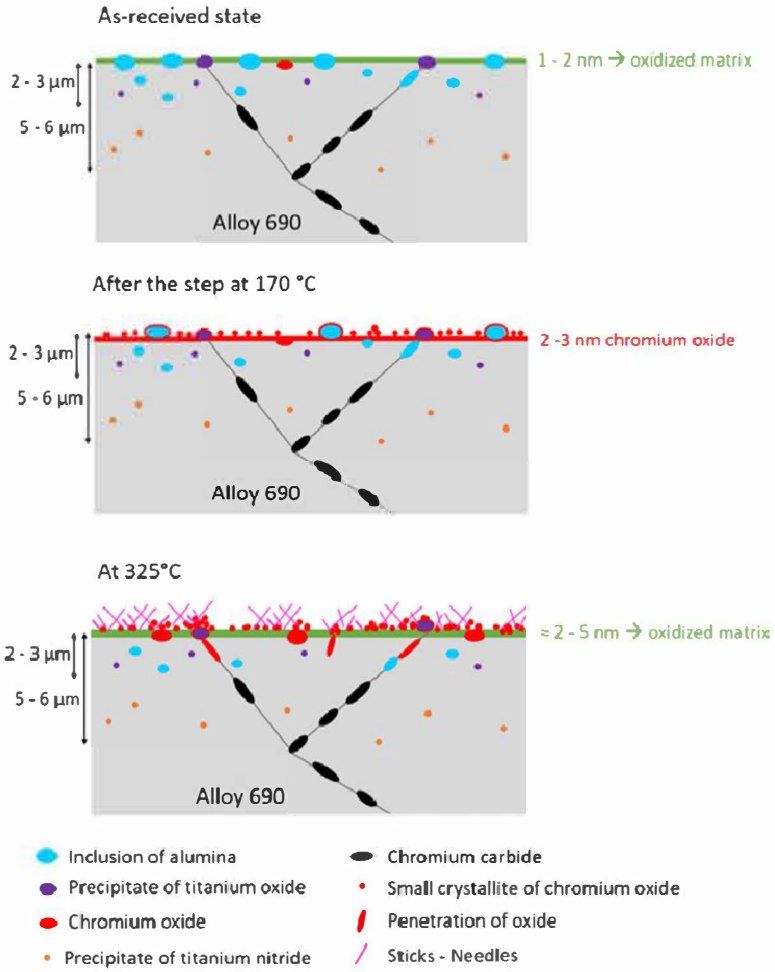

Figure 24. Schema of the oxide evolution and underlying material from the as-received state to the end of a simulate restart of reactor after steam generators replacement on the inner surface of a steam generator tube on alloy 690

the test conditions, in particular the conditions of circulation of the fluid inside the tube during the tests. In this study, the BOREAL loop reproduces at the tube scale a turbulent hydraulic regime, close to the conditions observed inside steam generator tubes of the primary circuit of PWRs. The flow rate is clearly higher than that usually practiced in tests of the literature, ranging from static condition in an autoclave to loop tests with laminar flow regimes of the order of 20 L/h maximum. These two major differences can largely explain the differences observed between the results of this study and those of the literature.

However, the results of this study are in agreement with those from a recent expertise on the internal surface of a 600TT alloy steam generator tube extracted from a nuclear power plant after 200 000 hours of service [27]. The SEM and TEM observations show an oxide consisting of an external layer, of approximately 5 μm, discontinuous and very porous interpreted as an exogenous oxide coming from the primary medium (more or less rich in iron and nickel). This layer would not be directly due to the oxidation of the tube. Then, an oxidation of the base metal over approximately 2 μm, rich in nickel, chromium and iron, with zones more or less enriched in one of these elements, is observed. In addition, partially oxidised particles of around 100 nanometers in the oxidised matrix layer are enriched in chromium. Particles enriched in titanium are also detected, which must come from the tube at the as-received state as noted in the context of this study. The thicknesses of the oxide layers are clearly greater (factor 100) than those observed in this study, but remain consistent with the durations of exposure in primary medium (200 times longer).

4.3. Oxidation and release mechanism

From the previous characterisations and the release kinetics, an oxidation and release mechanism during a restart of reactor after steam generators replacements can be proposed on Fig. 25. At the end of the step at 170°C, the relief of grain boundaries and steps is softened. The development of a layer mainly consisting of

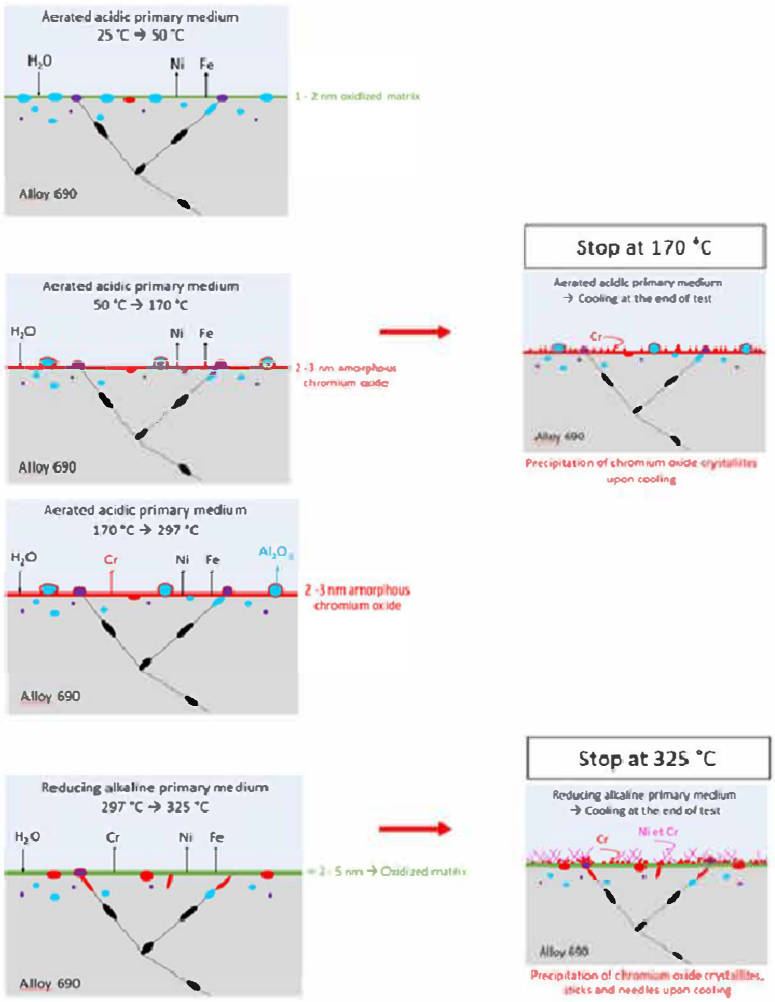

Figure 25. Schema of the oxidation and release mechanism on the inner surface of steam generator tube on alloy 690 during a restart of reactor after steam generators replacement

chromium oxide covers the initial relief by selective dissolution of nickel and iron. The solubility of metallic nickel, nickel oxide and iron oxide is greater at these temperatures than at 325°C. The diffusion phenomena are in the minority because the temperatures of first steps are too low to significantly activate diffusion. Therefore, the extreme surface is enriched in chromium and oxidizes by diffusion of OH^- hydroxyls anions present in the fluid. The kinetics of relaxation is then controlled by the kinetic limitation of solubilisation of corrosion products. The temperature of primary medium is not sufficient to dissolve the aluminium until this step. However, these Alumina inclusions are less deeply embedded than at the as-received state and surrounded of chromium oxide.

During the rise of temperature between 170°C and 297°C, the release strongly increases. The chromium oxide layer formed up to the 170°C step dissolves, it is not enough protective against oxidation and release. The Alumina inclusions also dissolve in the medium and contribute to the release measured experimentally in the test loop. Some areas such as grain boundaries, disturbed areas and stair nosing's contribute indeed mainly to release. With increasing temperature, the diffusion phenomena of metal cations migrating from the material to the fluid are activated. The OH^- hydroxyls anions will also diffuse more quickly at high temperature, which leads to the oxidation of the surface, hence the thin layer of oxidised matrix. Due to the disturbed microstructure of the as-received state, diffusion can also be promoted by short circuits (grain boundaries, dislocations, gaps).

The release kinetics present a pseudo-stationary regime at the end of the test, this implies that diffusion is the phenomenon limiting the release. In addition, a state of equilibrium is established between the limit diffusion layer and the oxide, explaining the relatively weak and constant kinetics of release at the end of the test.

The presence of needles and sticks composed of oxides/hydroxides of nickel and chromium, at the end of the test may be due to the precipitation of nickel and chromium in

solution during cooling on germs already present at high temperature. This formation would be explained by a phenomenon of dissolution/precipitation during the cooling of the fluid due to a locally supersaturation. With the turbulent hydraulic regime in the installation, it is unlikely that these elements will be able to resist at these hydraulic conditions.

This model couples the phenomena of oxidation and release, out of equilibrium, and it is based on industrial reality (materials and test conditions).

5. Conclusions

Sections of steam generator tubes were corroded in primary water conditions representative of restart conditions of a pressurized reactor after steam generators replacement. Kinetics of release kinetics of corrosion products were obtained using the BOREAL facility available at EDF R&D. These kinetic results associated to the characterisation of the inner surface of the tubes before and after the corrosion tests permit to propose an oxidation and release mechanism during a restart of reactor. This model is based on the following experimental observations:

The oxide layer at the as-received state is formed of a very thin layer (1 – 2 nm) of oxidised matrix, without specific enrichment.

During the restart, the most critical step for the release phenomenon is revealed from 170°C to 297°C.

Up to 170°C, a thin layer of amorphous chromium oxide is formed by selective dissolution of iron and nickel.

When the temperature rises, this chromium oxide layer is not stable enough to be protective and the diffusion phenomena are activated. At 325°C, the oxide does not exhibit any particular enrichment and corresponds to an oxidised metal layer, an equilibrium is established and the rate of release reaches a pseudo-stationary regime.

For a better understanding of the behaviour of steam generator tubes in terms of oxidation and release during a reactor restart after one operating cycle or several operating cycles, a program of release tests and characterisations is being developed. This program would be also include a study on the behaviour of steam generator tube during the reactor shutdown.

Data availability

The raw/processed data required to reproduce these findings cannot be shared at this time as the data also forms part of an ongoing study.

Declaration of Competing Interest

All the authors have approved the current manuscript and confirm that it has not been published elsewhere and that it is not under consideration for publication in any other journal.

We have not conflict of interest.

CRediT authorship contribution statement

Julie Flambard: Formal analysis, Validation, Visualization, Methodology, Data curation, Writing - original draft, Writing - review & editing. **Florence Carrette:** Funding acquisition, Resources, Project administration, Supervision, Writing - review & editing. **Carole Monchy-Leroy:** Funding acquisition, Resources, Project administration, Supervision, Writing - review & editing. **Eric Andrieu:** Methodology, Supervision, Validation, Conceptualization, Data curation, Writing - original draft, Writing - review & editing. **Lydia Laffont:** Funding acquisition, Methodology, Project administration, Supervision, Validation, Conceptualization, Data curation, Writing - original draft, Writing - review & editing.

Acknowledgments

Authors thank Valinox Nucléaire for supplying the SG tube with which the release tests were carried out and the CEMHTI laboratory of Orléans, France who performed the implantations of cobalt on SG tubes for the gammametric detection during release tests in the BOREAL loop.

Authors thank the team "Etude-Corrosion" of EDF R&D who performed the release tests in the BOREAL loop and thank as well the CIRIMAT, UMS Castaing at Toulouse, France, for the TEM characterisations and Science & Surface at Ecully, France, for ToF-SIMS analyses.

References

[1] H. Lefaix-Jeuland, L. Marchetti, S. Perrin, M. Pijolat, M. Sennour, R. Molins, Oxidation kinetics and mechanisms of Ni-base alloys in pressurised water reactor primary conditions: Influence of subsurface defects, Corrosion Science 53 (2011) 3914–3922.

[2] L. Guinard, O. Kerrec, D. Noel, S. Gardey, F. Coulet, Influence of initial surface condition on the release of nickel alloys in the primary circuit of PWRs, Nucl. Energy. 36 (1997) 19–27.

[3] M. Sennour, L. Marchetti, F. Martin, S. Perrin, R. Molins, M. Pijolat, A detailed TEM and SEM study of Ni-base alloys oxide scales formed in primary conditions of pressurized water reactor, Journal of Nuclear Materials 402 (2010) 147–156.

[4] F. Carrette, M.C. Lafont, G. Chatainier, L. Guinard, B. Pieraggi, Analysis and TEM examinations of corrosion scales grown on Alloy 690 exposed to pressurized water at 325°C: Corrosion scales on Alloy 690 grown in pressurized water, Surface and Interface Analysis 34 (2002) 135–138.

[5] F. Carrette, M.C. Lafont, L. Legras, L. Guinard, B. Pieraggi, Analysis and TEM examinations of corrosion scales grown on alloy 690 exposed to PWR environment, Materials at High Temperatures 20 (2003) 581–591.

[6] A. Machet, A. Galtayries, S. Zanna, L. Klein, V. Maurice, P. Jolivet, M. Foucault, P. Combrade, P. Scott, P. Marcus, XPS and STM study of the growth and structure of passive films in high temperature water on a nickel-base alloy, Electrochimica Acta 49 (2004) 3957–3964.

[7] J.E. Castle, H.G. Masterson, The role of diffusion in the oxidation of mild steel in high temperature aquous solutions, Corrosion Science 6 (1966) 93–104.

[8] Evans, Film formation on stainless steel in a solution containing chromic and sulphuric acids, Corrosion Science (1977) 105–124.

[9] J. Robertson, The mechanism of high temperature aqueous corrosion of stainless steels, Corrosion Science 32 (1991) 443–465.

[10] D.H. Lister, R.D. Davidson, E. McAlpine, The mechanism and kinetics of corrosion product release from stainless steel in lithiated high temperature water, Corrosion Science 27 (1987) 113–140.

[11] S. Gardey, Etude de la corrosion généralisée des alliages 600, 690 et 800 en milieu primaire - Contribution à la compréhension des mécanismes, Université Pierre et Marie Curie - Paris VI, 1998.

[12] F. Carrette, L. Guinard, B. Pierragi, kinetics of corrosion products release from Nickel-base alloys corroding in primary water conditions: a new modelling of release., in: Avignon, France, 2002.

[13] L. Guinard, D. Myszkiewicz, BOREAL: a new facility for studying the release of steam generator tubes., in: Bournemouth, England, 2000.

[14] F. Carrette, E. Riquelme, L. Guinard, J. Deshon, Impact of boron content of corrosion product release rate in PWRs, in: San Franciso, USA, 2004.

[15] L. Guinard, O. Kerrec, S. Gardey, D. Noel, Investigations for reducing the release of steam generator materials: experiments and modelling., in: Kashiwazaki, Japan, 1998.

[16] F. Carrette, F. Cattant, L. Legras, F. Bardet, M. Merrer, L. Guinard, Impact of the surface state of steam generator tubes on the release of corrosion Products in pressurized water reactors., in: Jeju Island, South Korea, 2006.

[17] L. Guinard, O. Lacroix, T. Sauvage, G. Blondiaux, Ultra thin layer activation by recoil implantation of radioactive heavy ions : applicability in wear and corrosion studies, Nuclear Instruments and Methods in Physics Research B122 (1997) 262–268.

[18] L. Legras, M.L. Lescoat, S. Jublot-Leclerc, A. Gentils, Optimisation of TEM preparation in metallic materials using low voltage ions, in: Proc. of the European Microscopy Congress, 2016.

[19] A. Mazenc, Caractérisation par TOF-SIMS des couches de passivation des tubes de générateur de vapeur en Alliage 690 pour l'industrie nucléaire : apport à la compréhension des mécanismes, Université Pierre et Marie Curie - Paris VI, 2013.

[20] D. Noel, L. Guinard, O. Kerrec, P. Le Bec, F. Schwoehrer, Contribution to the understanding of the surface condition effects on nickel alloys release and the role of the oxides., in: Ottawa, Japan, 1994.

[21] F. Carrette, Relâchement des produits de corrosion des tubes en alliage 690 de générateur de vapeur du circuit primaire des réacteurs à eau pressurisée, Polytechnic National Institut of Toulouse, 2002.

[22] F. Carrette, S. Leclercq, L. Legras, Characterisation of oxides formed on the internal surface of steam generator tubes in alloy 690 corroded in the primary environment of pressurised water reactors, in: Paris, France, 2012.

[23] F. Meng, J. Wang, E-H. Han, W. Ke, The role of TiN inclusions in stress corrosion crack initiation for Alloy 690TT in high-temperature and high-pressure water, Corrosion Science 52 (2010) 927–932.
[24] A.L. Bowman, G.P. Arnold, E.K. Storms, N.G. Nereson, The crystal structure of Cr23C6, Acta Crystallographica Section B 28 (1972) 3102.
[25] Y.B. Lee, J.S. Jang, D.H. Lee, I.H. Kuk, J. Kor, Inst. Met. Mater 35 (1997) 935.
[26] B Beverskog, I. Puigdomenech, Corrosion Nace vol.55 (11) (1999) 1077–1086.
[27] C.G. Panait, M. Boccanfuso, L. Legras, Y. Thebault, S. Miloudi, F. Carrette, B. Martin-Cabanas, O. Alos-Ramos, Microstructural investigations of a steam generator tube oxide after zinc injection, in: Avignon, France, 2018.